

Effect of two-dimensional parity symmetry breaking in Aharonov-Bohm interference phenomena

Yuantao Xie^a, J. J. Heremans^a, and M. B. Santos^b

^aDepartment of Physics, Virginia Tech, Blacksburg, VA, USA; ^bHomer L. Dodge Department of Physics and Astronomy, University of Oklahoma, Norman, OK, USA

ABSTRACT

The quantum-mechanical dephasing effect of a two-dimensional parity symmetry breaking is demonstrated in a solid-state quantum-coherent mesoscopic ring interferometer. The interferometer, fabricated on an InGaAs/InAlAs heterostructure, shows Aharonov-Bohm oscillations under magnetic fields at low temperatures. Under asymmetric bias voltage on side-gates, a weakening of the Aharonov-Bohm oscillations is observed. The weakening corresponds to an effective dephasing under two-dimensional parity symmetry breaking by the applied electric field, and is interpreted as a counterpart to the weakening observed under time-reversal symmetry breaking by a magnetic field.

ARTICLE HISTORY

Accepted 15 January 2016

KEYWORDS

Aharonov-Bohm phase; parity symmetry; quantum coherence; mesoscopic physics; InGaAs; interferometer

The quantum-mechanical effects of broken symmetries, including time-reversal symmetry and parity symmetry, can be studied experimentally via the resulting quantum dephasing in mesoscopic solid-state systems. In the present work, Aharonov-Bohm (AB) oscillations [1–5] are used to study dephasing under a broken parity symmetry induced in the respective arms of a quantum ring interferometer. The oscillations appear in the low-temperature electrical conductance of the interferometer structure versus applied magnetic field B . Symmetries play an important role in solid-state phenomena, among others in the categorization of ferroic orders (ferroelectric, ferromagnetic, multiferroic, and others) [6]. The work below focuses on the foundational nature and geometrical aspects of mirror symmetry breaking in a quantum mechanically coherent entity. Previously, the effects of time-reversal symmetry breaking by magnetic fields were studied in a similar structure, and the geometrical aspects, described by a magnetic length, of time-reversal symmetry breaking were emphasized [7]. The mirror symmetry manipulated in the present work is a two-dimensional parity symmetry, and its study in quantum phenomena is justified due to the role CPT (charge conjugation-parity-time) symmetry assumes in quantum physics.

CONTACT J. J. Heremans  heremans@vt.edu

Color versions of one or more of the figures in the article can be found online at www.tandfonline.com/ginf.

© 2016 Taylor & Francis Group, LLC

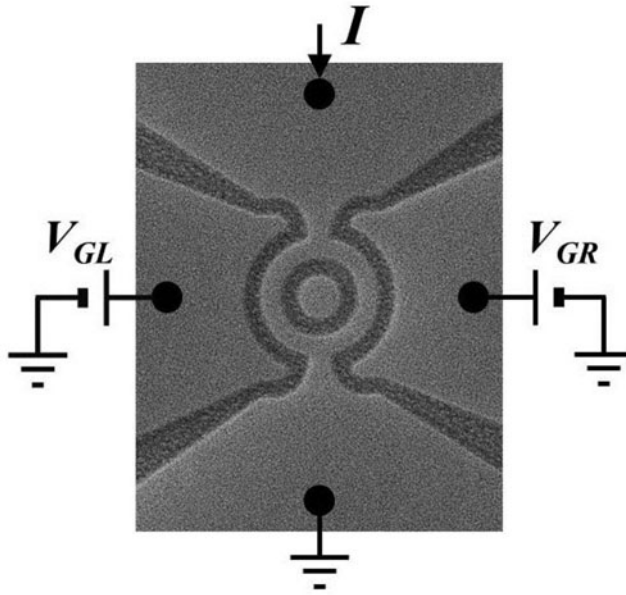


Figure 1. Scanning electron micrograph of the side-gated ring interferometer, with schematic measurement setup. Conducting areas are lighter in shade, etched non-conducting trenches darker. The ring's average radius is 650 nm.

Low-temperature mesoscopic quantum electronic transport on a narrow-gap semiconductor InGaAs quantum well is used, where the interferometer length scale is comparable to the spin coherence and quantum phase coherence lengths in the material. Hence phenomena relying on a retention of quantum coherence can be observed (for an example, see [8]). AB oscillations are evidence of the nonlocal quantum nature of mesoscopic conductance phenomena, and are caused by quantum interference between partial waves traveling in spatially separate interferometer arms when a magnetic flux φ threads between the two arms [2,7]. The two partial waves accumulate a total relative AB phase of 2π if they traverse separate trajectories enclosing a magnetic flux quantum h/e (where $h = 2\pi\hbar$ with \hbar the Planck constant and e the electron charge). Due to alternatively constructive and destructive quantum interference, the transmittance and conductance of the interferometer then oscillate in B with a periodicity corresponding to $\varphi = h/e$.

Figure 1 shows a scanning electron micrograph of the ring interferometer studied in this work. Conducting areas, including the ring, are defined by lighter-colored areas, whereas darker areas are depleted of carriers (the innermost lighter-colored disc has no function). The ring has a lithographic average radius $r = 650$ nm, and the arms have lithographic width 300 nm (the conducting width is narrower due to edge depletion [2]). A variable uniform B is applied over the ring area, while the resistance R of the ring is measured using low-frequency ac lock-in four-terminal measurements. Figure 1 indicates the direction of the ac excitation current through the ring, kept at 20 nA to prevent carrier heating. The expected AB oscillation period in B , given by $(h/e)/(\pi r^2)$, is 3.1 mT for the given r . Figure 1 also shows two side-gates

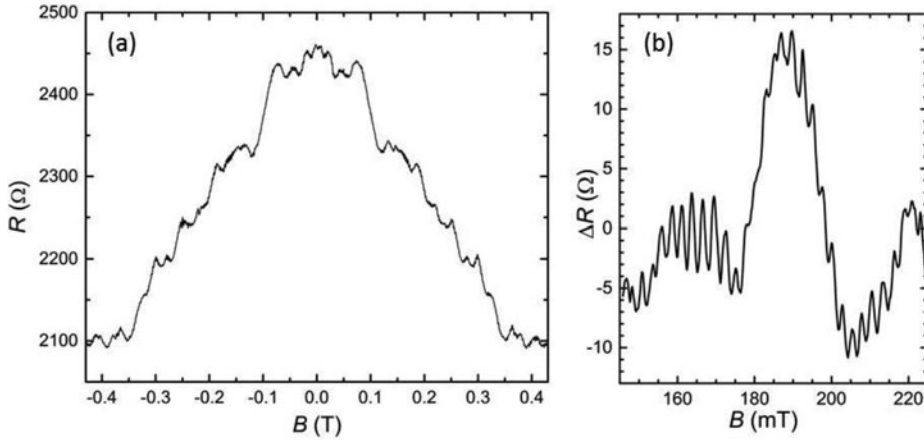


Figure 2. (a) Resistance R of the ring measured vs B normal to the surface, at $T = 0.38$ K and $V_{GL} = V_{GR} = 0$. Aharonov-Bohm oscillations (amplitude ~ 10 Ω not fully resolved in this wide-range figure) appear, modulated in amplitude, on top of a resistance background and universal conductance fluctuations. (b) High-resolution zoom-in on the region $145 \text{ mT} < B < 225 \text{ mT}$, showing R with the magnetoresistance background removed (ΔR) to emphasize the Aharonov-Bohm oscillations, with measured periodicity 2.9 mT.

[9,10] defined by the lighter-colored areas flanking the ring, and separated from the conducting arms by an insulating trench of width 250 nm. To each side-gate a voltage bias can be applied referred to the ring potential (or ground), V_{GL} or V_{GR} . The side-gate voltages V_{GL} and V_{GR} create an electric field (with dominant component in the plane of the ring), penetrating respectively the left or right interferometer arm. The difference in electric fields over the left and right interferometer arms breaks the mirror symmetry or two-dimensional parity symmetry of the structure. As an example, Fig. 2(a) shows the measured resistance of the ring ($V_{GL} = V_{GR} = 0$) at a temperature $T = 0.38$ K, as function of B . On top of the classical ring resistance of 2450 Ω ($B = 0$) and of a long-period magnetoresistance structure due to universal conductance fluctuations [11], pronounced AB oscillations appear. The oscillations, appearing *e.g.* strongly at ± 0.05 T, ± 0.16 T, ± 0.24 T, ± 0.41 T, *etc.*, are non-uniform and modulated in amplitude as expected [2,12–14]. Figure 2(b) shows a zoom-in at higher-resolution, where a magnetoresistance background has been removed to accentuate the AB oscillations. The AB periodicity in Figs. 2(a) and 2(b) is 2.9 mT, in excellent agreement with the predicted periodicity of 3.1 mT.

The interferometer in Fig. 1, yielding a periodicity of h/e due to the AB phase as seen in Fig. 2, is a Mach-Zehnder interferometer, relying on spatially separate interferometer arms [7]. A spatial asymmetry between the two arms, either intentional or originating in fabrication and materials imperfections, can give rise to an additional phase shift between the two partial waves, possibly leading to dephasing and a decrease in the oscillations' visibility. It is readily seen that in the extreme asymmetric case of elimination of one of the arms, or for a side-gate voltage sufficiently negative to deplete one of the arms of electrons, the oscillations will disappear.

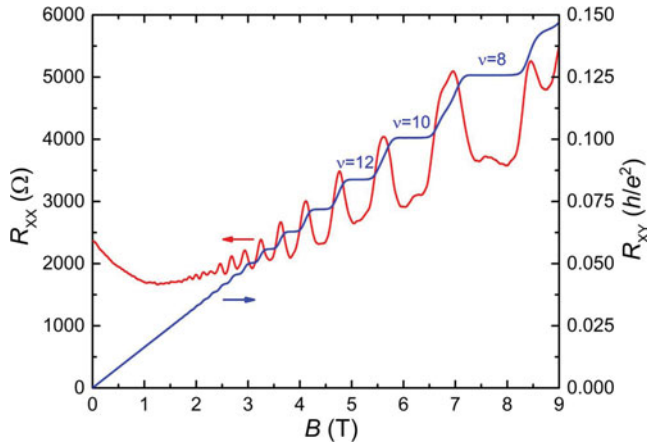


Figure 3. Left axis: resistance R ($= R_{XX}$) of the ring vs B up to the integer quantum Hall regime, at $T = 0.38$ K and $V_{GL} = V_{GR} = 0$. Shubnikov-de Haas oscillations appear for $B < \sim 3$ T, developing in integer quantum Hall features. Right axis: Hall resistance R_{XY} over unpatterned sample regions, showing integer quantum Hall plateaux, labeled with the Landau level filling factor ν .

The AB ring was fabricated on an $\text{In}_{0.64}\text{Ga}_{0.36}\text{As}/\text{In}_{0.45}\text{Al}_{0.55}\text{As}$ heterostructure by electron beam lithography and reactive ion etching (ICP-RIE). Electrons in the heterostructure form a two-dimensional electron system (2DES) located in a 10 nm wide $\text{In}_{0.64}\text{Ga}_{0.36}\text{As}$ quantum well at a depth 50 nm from the surface. The 2DES density $N_S = 1.48 \times 10^{16} \text{ m}^{-2}$ (resulting in a Fermi wavelength of 21 nm) and the mobility is $7.8 \text{ m}^2/\text{Vs}$ at 0.4 K, yielding in a 2DES resistivity $54 \text{ } \Omega/\square$. With non-parabolicity in the conduction band, the mean free path amounts to $3.2 \text{ } \mu\text{m}$, signifying the interferometer operates in the ballistic regime. The quality of the heterostructure is evident from Fig. 3, which shows the Hall resistance R_{XY} and the longitudinal resistance R_{XX} as measured over the ring ($T = 0.38$ K) up to high B . The R_{XY} trace shows integer quantum Hall plateaux, up to Landau level filling factor $\nu = 8$. The R_{XX} trace also shows integer quantum Hall effect features at higher B . Yet minima do not reach $R_{XX} = 0$ since R_{XX} was obtained over the mesoscopic ring in which opposite edge states communicate and hence backscatter [15]. At lower B the R_{XX} trace contains Shubnikov-de Haas oscillations. The value for N_S was obtained from both Shubnikov-de Haas and Hall data.

Figure 4 show the ring resistance R vs B obtained under asymmetric side-gate biasing, for $-75 \text{ mT} < B < 75 \text{ mT}$. AB oscillations of amplitude $\sim 4 \dots 10 \text{ } \Omega$, on a background of $\sim 2800 \dots 3300 \text{ } \Omega$, are clearly visible in specific regions of B (amplitude modulations are also present, as discussed in [2]). In these experiments, V_{GL} is varied from 1.8 V to -1.2 V, while $V_{GR} = 0$. The values $R(B = 0)$ in Fig. 4 demonstrates that the ring becomes more resistive at more negative V_{GL} as expected from a depletion of electrons in the left arm at more negative side-gate voltages. The background magnetoresistance, partially due to universal conductance fluctuations, also varies with V_{GL} since the mesoscopic representation of the sample changes for different V_{GL} . A slight hysteresis in both V_{GL} and V_{GR} occurs as well, but has no impact on the AB oscillation data. In Fig. 4 overall strongest AB oscillations in R occur

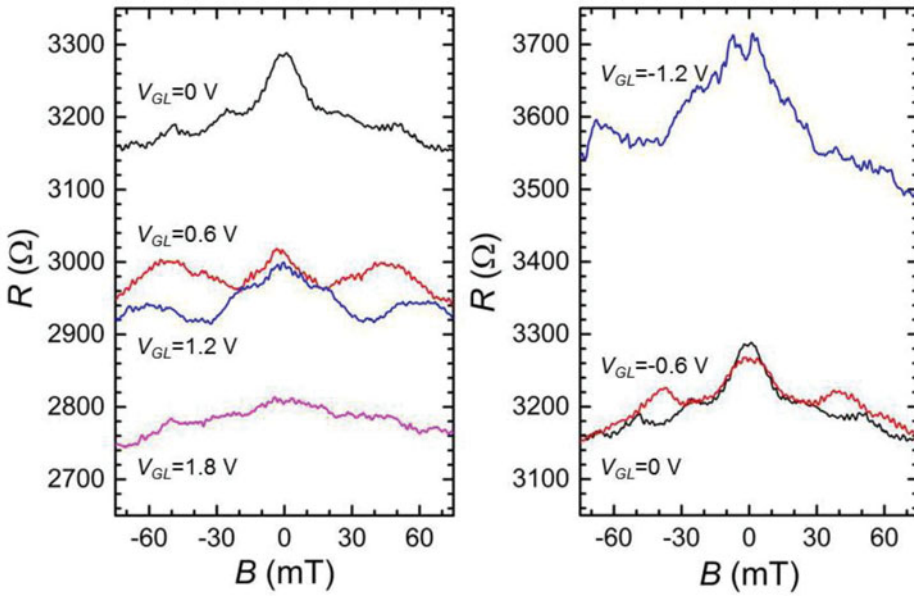


Figure 4. Resistance R of the ring measured vs B at $T = 0.38$ K under asymmetric side-gate bias, with V_{GL} as indicated and $V_{GR} = 0$. The left panel shows data for $V_{GL} \geq 0$, the right panel for $V_{GL} \leq 0$. Aharonov-Bohm oscillations are visible in all traces.

for $V_{GL} = V_{GR} = 0$, the mirror-symmetric case. For $V_{GL} = 0.6$ V with $V_{GR} = 0$ the oscillations are slightly diminished, whereas for $V_{GL} = 1.8$ V with $V_{GR} = 0$ the oscillations are clearly diminished. For $V_{GL} = -1.2$ V with $V_{GR} = 0$ the oscillations have weakened significantly. **Figure 5** contains a quantification of the observations relating to **Fig. 4**, with the maximum observed oscillation amplitude over -75 mT $< B < 75$ mT, plotted vs V_{GL} ($V_{GR} = 0$). The plotted amplitude forms an approximate measure of the strength of the quantum interference effect in the presence of the inevitable amplitude modulation. The strongest oscillations occur for $V_{GL} =$

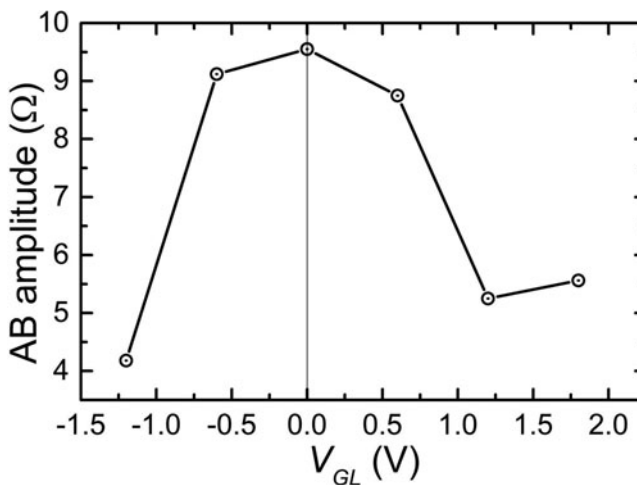


Figure 5. The maximum amplitude of Aharonov-Bohm oscillations observed in the data of **Fig. 4**, as function of V_{GL} (with $V_{GR} = 0$).

$V_{GR} = 0$, with visibility falling for both $V_{GL} < 0$ and $V_{GL} > 0$. The fall-off is stronger for $V_{GL} < 0$, likely due to secondary effects of electron depletion in the left arm for $V_{GL} < 0$. It is the maximum in oscillation strength observed for $V_{GL} = V_{GR} = 0$, the symmetric case, which forms the main result of the study.

The breaking of the two-dimensional parity symmetry hence results in a fading of the quantum interference signal, and thus effectively in a dephasing effect for the system. The Mach–Zehnder interferometer used in the experiment is specifically sensitive to spatial asymmetry, relying on spatially separate paths. The Mach–Zehnder interferometer can be contrasted with interferometer arrays wherein the signal arises from time-reversed paths, and such arrays hence show a sensitivity to time-reversal symmetry breaking, *e.g.* originating in B penetrating the arms [7]. The present experiment constitutes a dual to such interferometric measurements of time-reversal symmetry breaking, as in the present experiment an electric field breaks two-dimensional parity symmetry in an interferometer specifically sensitive to parity symmetry. The experiment shows that, in analogy to the effect of time-reversal symmetry breaking by a magnetic field, a breaking of parity symmetry by an electric field leads to an effective quantum dephasing.

In conclusion, a mesoscopic ring Mach-Zehnder interferometer with side-gates was fabricated on an InGaAs/InAlAs heterostructure. Aharonov-Bohm quantum interference oscillations in the interferometer are measured at 0.38 K under applied magnetic fields, to study the dephasing effect of spatial symmetry breaking over the ring. The side-gates allow application of transverse electric fields, and under asymmetric bias they allow a breaking of the mirror or two-dimensional parity symmetry of the device. It is observed that indeed the amplitude of the Aharonov-Bohm oscillations weakens under asymmetric side-gate bias, confirming the effective dephasing effect of a breaking of two-dimensional parity symmetry. The experiments form a dual counterpart to previous experiments studying the dephasing effects of time-reversal symmetry breaking and substantiate the non-trivial consequences of symmetry breaking in quantum-coherent structures.

Acknowledgments

The work was supported by the U.S. Department of Energy, Office of Basic Energy Sciences, Division of Materials Sciences and Engineering under award DOE DE-FG02-08ER46532 (JJH: experiment design, sample fabrication, and measurement), and by the National Science Foundation under award NSF DMR-1207537 (MBS: heterostructure growth).

References

1. Y. Aharonov, and D. Bohm “Significance of electromagnetic potentials in quantum theory”. *Phys. Rev.* **115**, 485–491 (1959).
2. S. L. Ren, J. J. Heremans, C. K. Gaspé, S. Vijayaragunathan, T. D. Mishima, and M. B. Santos “Aharonov–Bohm oscillations, quantum decoherence and amplitude modulation in mesoscopic InGaAs/InAlAs rings”. *J. Phys.: Cond. Mat.* **25**, 435301 (7pp) (2013).

3. S. Washburn, and R. A. Webb “Aharonov-Bohm effect in normal metal, quantum coherence and transport”. *Adv. Phys.* **35**, 375–422 (1986).
4. S. Oliaru, and I. I. Popescu “The quantum effects of electromagnetic fluxes”. *Rev. Mod. Phys.* **57**, 339–436 (1985).
5. A. G. Aronov, and Yu. V. Sharvin “Magnetic flux effects in disordered conductors”. *Rev. Mod. Phys.* **59**, 755–779 (1987).
6. S.-W. Cheong, and M. Mostovoy “Multiferroics: a magnetic twist for ferroelectricity”. *Nat. Mater.* **6**, 13–20 (2007).
7. S. L. Ren, J. J. Heremans, C. K. Gaspe, S. Vijayaragunathan, T. D. Mishima, and M. B. Santos “Determination of time-reversal symmetry breaking lengths in an InGaAs Sagnac interferometer array”. *J. Phys.: Cond. Mat.* **27**, 185801 (7pp) (2015).
8. C. Texier, P. Delplace, and G. Montambaux “Quantum oscillations and decoherence due to electron-electron interaction in metallic networks and hollow cylinders”. *Phys. Rev. B* **80**, 205413 (1–32) (2009).
9. M. Kohda, S. Nakamura, Y. Nishihara, K. Kobayashi, T. Ono, J. Ohe, Y. Tokura, T. Mineno, and J. Nitta “Spin-orbit induced electronic spin separation in semiconductor nanostructures”. *Nat. Commun.* **3**, 1082 (8pp) (2012).
10. L. P. Rokhinson, L. N. Pfeiffer, and K. W. West “Spontaneous spin polarization in quantum point contacts”. *Phys. Rev. Lett.* **96**, 156602 (1–4) (2006).
11. M. Rudolph, and J. J. Heremans “Spin-orbit interaction and phase coherence in lithographically defined bismuth wires”. *Phys. Rev. B* **83**, 205410 (1–6) (2011).
12. M. A. Castellanos-Beltran, D. Q. Ngo, W. E. Shanks, A. B. Jayich, and J. G. E. Harris “Measurement of the full distribution of persistent current in normal-metal rings”. *Phys. Rev. Lett.* **110**, 156801 (1–5) (2013).
13. L. C. Mur, C. J. P. M. Harmans, and W. G. van der Wiel “Competition between h/e and $h/2e$ oscillations in a semiconductor Aharonov-Bohm interferometer”. *New J. Phys.* **10**, 073031 (16pp) (2008).
14. F. Nichele, Y. Komijani, S. Hennel, C. Gerl, W. Wegscheider, D. Reuter, A. D. Wieck, T. Ihn, and K. Ensslin “Aharonov-Bohm rings with strong spin-orbit interaction: the role of sample-specific properties”. *New J. Phys.* **15**, 033029 (15pp) (2013).
15. V. J. Goldman, J. Liu, and A. Zaslavsky “Electron tunneling spectroscopy of a quantum antidot in the integer quantum Hall regime”. *Phys. Rev. B* **77**, 115328 (1–10) (2008).